Structure of submonolayer oleic acid coverages on inorganic aerosol particles: evidence of island formation

Eva R. Garland,[a] Elias P. Rosen,[a] Laura I. Clarke*[b] and Tomas Baer*[a]

Received 21st November 2007, Accepted 14th March 2008
First published as an Advance Article on the web 14th April 2008
DOI: 10.1039/b718013f

A series of submonolayer deposition studies of oleic acid on both hydrophobic and hydrophilic surfaces has shown that oleic acid self-associates into islands rather than uniformly covering the surfaces. The studies were performed by vapor deposition on 1.6 μm diameter polystyrene aerosol particles as well as on polystyrene and silica surfaces. The surfaces were investigated by scanning electron microscopy (SEM), atomic force microscopy (AFM), ellipsometry and contact-angle goniometry. After timescales of minutes to hours of vapor deposition at 70 °C, the oleic acid arranged itself in the form of islands with diameters of about 100 nm. Many of the islands are 25–30 Å high, suggesting that the oleic acid sits vertically on the surface. The surface structure of oleic acid on particles is expected to impact on several atmospherically relevant properties such as the reactivity of the oleic acid and the hygroscopicity of the particles.

Introduction

Recent field measurements have shown that internally mixed aerosol particles containing organic species comprise a large fraction of aerosol particles in the atmosphere.[1–5] Mixed organic–inorganic particles may form when low-volatility gaseous organic compounds condense onto pre-existing liquid or solid particles.[6–8] These organic coatings can dramatically alter the properties of the coated particles including their toxicity, their ability to act as cloud condensation nuclei and their reactivity.[9,10]

When an organic film covers the particle, it may serve as either an inert or a reactive barrier to diffusion of gases. Studies have shown that monolayer coverages of organic acids on aqueous sea-salt aerosol particles inhibit the uptake of N_2O_5 by a factor of 3–4.[11,12] The impact of an organic coating on a particle's properties is dependent on the structure of the coating. For example, the hygroscopicity of aqueous sulfuric acid particles was shown to be inhibited more strongly by a surface coating of linear, closely packed organic acids than by non-linear organic acids.[13]

The surface composition and structure of the core particle can influence the arrangement of the organic film on the particle surface. Considerable attention has been placed on the organizational effects of aqueous–organic systems. Ellison *et al.*[14] hypothesized that an organic acid layer on an aqueous particle forms an inverted micelle with the hydrophilic acid group facing the water core and the hydrophobic part facing outward. This effectively changes the surface of the particle from hydrophilic to hydrophobic, resulting in a decrease in its ability to act as a cloud-condensation nucleus (CCN). The presence of other organic species on the particle can also impact the stability and evaporation rate of surface organics.[15]

The reactivity of organic molecules in particles can be influenced by particle morphology, as has been demonstrated in several studies of the reaction of oleic acid particles with ozone. Ozonolysis of oleic acid in pure particles occurs much more quickly than is observed in ambient particles.[16,17] Analysis of internally mixed oleic acid particles with other organic species indicates that the rate is affected by both the composition and the morphology of the particle.[18] A related finding by Nash *et al.*[19] found that the oxidation rate by ozone of aerosol particles consisting of 10% myristic acid in oleic acid dropped significantly relative to pure oleic acid because the 2% solid phase arranged itself to form a monolayer of myristic acid around the liquid droplet, thereby reducing the diffusion rate of ozone into the particle.

The deposition of oleic acid onto substrates from solution has been the subject of a significant amount of research. Blyholder *et al.*[20] obtained infrared spectra for oleic acid adsorbed onto silica gel from a solution of oleic acid and hexane. They report three different adsorption structures: singly and doubly hydrogen-bonded chemisorption and physically adsorbed dimeric oleic acid. Another study using the same coating method noted that the –OH infrared signal of silica nanoparticles first decreased linearly as a function of the percent composition of oleic acid in solution and then leveled off at higher oleic acid percentage compositions.[21] Liu *et al.*[22] found that a basic solution was necessary in order for chemisorption to occur for oleic acid deposited on γ-alumina powder. Since the nature of the substrate–surface interaction can be influenced by the solution composition, studies employing solution deposition may not provide good models for understanding organic coatings on aerosol particles. Deposition in the atmosphere involves direct, solvent-free condensation of organic species onto substrates and so vapor deposition is a better technique for replicating atmospheric conditions.

Although organic acids make up a significant fraction of the total organic matter in aerosol particles, few studies have examined their adsorption *via* vapor deposition onto solid

[a] *Chemistry Department, University of North Carolina, Chapel Hill, NC 27599-3290, USA*
[b] *Physics Department, North Carolina State University, Raleigh, NC 27695-8202, USA*

inorganic particles. Katrib *et al.*[23,24] coated polystyrene latex spheres with oleic acid, monitored the change in aerodynamic diameter and density of the particles as they reacted with ozone, and detected the products of the reaction. The uptake of organic acids on soot particles has also been investigated.[25]

The kinetics of ozonolysis of oleic acid particles has been the subject of significant work in our lab, and we have recently extended our studies to oleic acid coated on core inorganic substrates. Our initial experiments on these coated particles suggested that the aerodynamic diameter did not increase with small coverages of oleic acid. Also, the rate of ozonolysis of the oleic acid on the particles remained constant over a range of submonolayer coverages. These studies motivated us to characterize the morphology of the oleic acid vapor-deposited on both polar (silica) and nonpolar (polystyrene) substrates. We imaged both silica and polystyrene particles coated with oleic acid using scanning electron microscopy (SEM). We further investigated the structure of oleic acid vapor-deposited on flat surfaces of silica and polystyrene with a combination of analytical tools including atomic force microscopy (AFM), ellipsometry and contact-angle goniometry. Our studies investigate submonolayer coverages of oleic acid on substrates, which is notably different from the studies of Katrib *et al.*[23,24] that examined many monolayers of oleic acid on polystyrene latex (PSL) particles. Additionally, the particles examined by Katrib *et al.* were significantly smaller (100 nm) than those used in our study.

We show that oleic acid forms "islands" on both polar silica substrates and nonpolar polystyrene substrates. For our submonolayer coverages, we define island formation as the congregation of oleic acid molecules on the surface, as opposed to even dispersion. Such terminology is consistent with that used in the literature.[26]

Experimental

Sample preparation

The core particles used in this study consisted of nonporous silica particles and polystyrene latex spheres (PSLs) of 1.6 micron diameter (Duke Scientific, United States). The particles were suspended in a 50 : 50 water–methanol solution and atomized with a commercial atomizer (Model 3076, TSI, United States). The atomized stream passed through a heated tube and a diffusion dryer to remove the solvent. For coating experiments, particles were sent through an oven containing oleic acid heated to 70 °C. Aerodynamic size was obtained with an Aerodynamic Particle Sizer (Model 3321, TSI, United States).

Flat silica substrates were prepared by treating a silicon(100) wafer with UV–O_3 in a commercial instrument followed by washing with de-ionized water. Ellipsometry measurements indicate that the native SiO_2 coating on the silicon wafer was ~10–15 Å thick after this cleaning procedure. A flat polystyrene surface was prepared by spin-coating polystyrene dissolved in toluene on a silica substrate followed by annealing for 12–24 h at 130 °C.[27]

Oleic acid was deposited on the silica and polystyrene surfaces *via* vapor deposition in an oven at 70 °C. The oleic acid was pre-heated for several minutes and then the substrate was placed upside-down on top of a beaker containing a reservoir of liquid oleic acid. A second, larger, inverted beaker covered the setup in order to contain the oleic acid vapor.

Surface characterization

SEM. Particles were collected on a stub, and images were taken with a Hitachi S-4700 SEM (Japan). For the images presented here, particles were sputter-coated with 2 nm of an Au/Pd alloy (60 : 40) prior to analysis. Au/Pd coatings are commonly used for SEM analysis of nonconducting samples since a thin layer of the alloy provides a smooth coating. In order to assess whether the Au/Pd coating altered the surface features, images were also taken without sputter-coating. A similar surface structure was observed for both the sputter-coated and the non-sputter-coated samples. However, charging effects decreased the quality of the non-sputter-coated images, and so we show only the sputter-coated images in this work.

AFM. Measurements were taken with an Autoprobe M5 AFM (Thermomicroscopes, United States). All images were taken using the non-contact mode and tips had a force constant of 5 N m^{-1} and a reported radius of curvature of 40 nm. We typically used a gain of 0.2, a drive of 80% and a set point of −0.02 μm. Image backgrounds were flattened with AutoProbe Image software, which is supplied with the AFM instrument. A computer program was written to determine the number of islands and peak heights at a variety of deposition times. This program selected for islands that were a minimum of 10 Å above the background signal.

Ellipsometry. Data were taken with an Auto EL null ellipsometer (Rudolph Research, United States). Ellipsometry provides a measurement of the average thickness of a film based on the change in polarization of reflected light, assuming the index of refraction of the coating is known. An index of refraction of 1.46 was used for all measurements. Conveniently, this is the index of refraction for both silica and for oleic acid. The index of refraction for bulk polystyrene is 1.58, and is a sharp function of orientation of the polymer chains and of film thickness.[28] Since we were only concerned with the approximate thickness of the polystyrene layer, no effort was made to correct for its index of refraction.

Contact-angle goniometry. A droplet of water was pipetted onto a bare or coated silica surface. A picture of the water droplet on the surface was taken and the angle between the surface and the droplet was measured with image analysis software.

Computational approach. A DFT calculation was carried out using the Gaussian 2003 system of programs.[29] The optimized geometry of the oleic acid molecule was obtained using the B3LYP function and the 6-311 + + g(d,p) basis set.

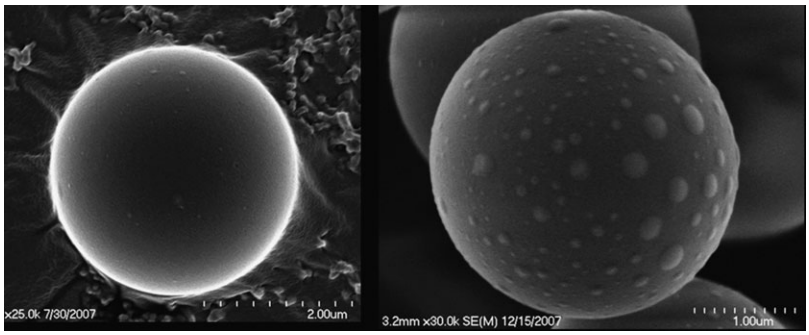

Fig. 1 SEM images of polystyrene latex spheres uncoated (left) and coated with oleic acid (right).

Results and discussion

Oleic acid coatings on particles

SEM images of 1.6 micron PSL particles both uncoated and coated with oleic acid are shown in Fig. 1. The coated particles show more structure than the uncoated particles, suggesting that the surface coating may be uneven. The image contrast is a result of the dependence of the number of secondary electrons and backscattered electrons on the topology of the surface. We also took SEM images of uncoated and coated silica particles, but the rough surface of the uncoated particles made it more difficult to distinguish differences in morphology between the coated and uncoated silica particles.

The SEM results motivated us to investigate further the morphology of oleic acid coatings on polar (silica) and non-polar (polystyrene) surfaces. In order to take advantage of a variety of analytical techniques, and to better quantitate the results, we performed the remainder of the experiments using flat substrates with a surface layer of SiO_2 or polystyrene (see Experimental). A flat substrate is a good approximation for the micron-sized particles used in this study since the particles' radius of curvature is large compared to the size of an oleic acid molecule. The similarity in our AFM results on flat surfaces (see below) and our SEM results on particles further support this assumption. Additionally, we found that SEM images of oleic acid on the flat substrates were similar to those of the coated particles.

Oleic acid coatings on silica surfaces

Ellipsometry was used to measure the average thickness of the oleic acid coating as a function of deposition time on silica substrates, and the results are shown in Fig. 2. Although the dynamics of the coating process are complex, we perform a simplified analysis in order to predict the coating time necessary for monolayer formation. The distance between the oleic acid reservoir and the substrate surface was approximately 2 cm. Based on the Chapman–Enskog equation, the diffusion coefficient of oleic acid in air at 70 °C is 0.043 $cm^2\ s^{-1}$ and so the time for a molecule to diffuse from the surface of the oleic acid reservoir to the substrate is 46 s. The oleic acid vapor pressure at 70 °C is 3–4 $\times\ 10^{-5}$ Torr,[30,31] corresponding to 1 $\times$ 10^{12} molecules cm^{-3}. The surface area occupied by each oleic acid molecule if the molecules are stacked vertically is 21 $Å^2$.[32] If we assume that every time an oleic acid molecule deposits on the surface of the substrate another oleic acid molecule is released from the reservoir, then it would require approximately 2.5 h for a monolayer to travel from the surface of the oleic acid reservoir to the surface of the substrate.

We note that the thickness of the oleic acid layer increases rapidly at first and then more slowly at longer times. Thus, the experimentally observed time for monolayer formation is significantly longer than our calculated value of 2.5 h. The similarity of the coating on both silica and polystyrene (see below) surfaces suggests that preferential chemisorption at defect sites is not responsible for the dynamics. The rate of deposition slows before a significant fraction of the surface is covered by oleic acid and so the dynamics cannot be explained by a model in which oleic acid that is already on the surface is blocking other molecules from adsorbing (as would be expected for chemisorption). Therefore, re-evaporation of the oleic acid from the substrate surface most likely accounts for the non-linear shape of the curve in Fig. 2. At short times, the rate of coverage is nearly linear with time since much more oleic acid is adsorbing to rather than desorbing from the surface; however, at longer times, a significant fraction of the adsorbed oleic acid is desorbing from the surface and so the growth is no longer linear. This is consistent with a growth model reported by Kubono *et al.*[33] for films involving cluster formation.

Also plotted in Fig. 2 is the contact angle of a water drop on the surface, as obtained with contact-angle goniometry. The contact-angle measurements scale with the amount of coating, indicating that the surface is becoming more hydrophobic.

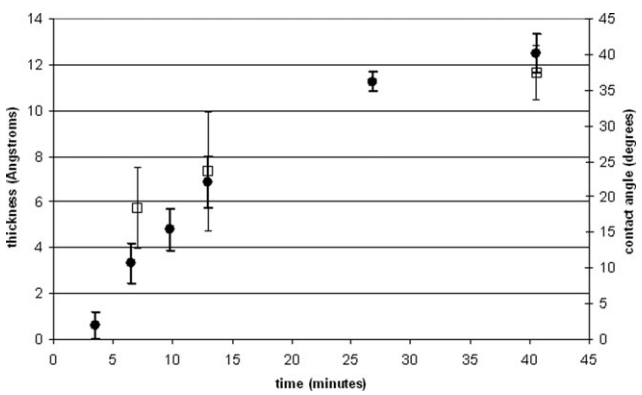

Fig. 2 Deposition of oleic acid on silica measured with ellipsometry (solid circles) and contact-angle goniometry (open squares). All error bars represent one standard deviation of the measurements.

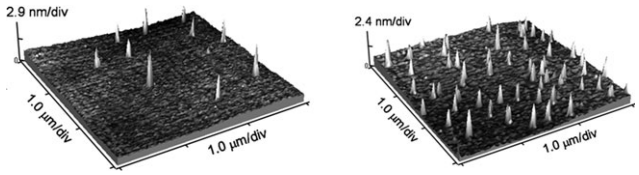

Fig. 3 AFM images of oleic acid on a silica surface at a short deposition time (left) and a longer deposition time (right). The number of islands increases with deposition time, but their peak heights are similar in both images.

AFM images of the silica substrates exposed to different amount of oleic acid are shown in Fig. 3. Both images show that oleic acid forms islands on the silica surface rather than coating the surface evenly. The diameter of these islands is approximately 100 nm, a value that is an upper limit because the resolution may be limited by the tip radius of curvature.

We further examined the dynamics of island formation by comparing the number of islands and peak heights at a variety of deposition times. A histogram of the results for a 17.5 h deposition are shown in Fig. 4 and a summary of the statistics for three different deposition times is presented in Table 1. We note that although the number of islands increases with deposition time, the mean diameter of these islands remains around 100 nm.

For all deposition times, the mean height of the islands is approximately 28 Å. Iwahashi *et al.*[32] have measured the length of oleic acid molecules in the liquid state to be 23.8 Å. We performed a density functional theory (DFT) geometry optimization that resulted in a calculated length of 21.2 Å. The island heights observed using AFM of approximately 28 Å are consistent with the measured and calculated lengths of the oleic acid molecule, and the roughness of the silica surface may account for the small difference in values. Therefore, it is likely that the observed islands consist of a single monolayer of oleic acid molecules oriented such that their long axis is perpendicular to the substrate surface.

The AFM results cannot distinguish whether islands are forming directly on the silica or if they exist on top of an already-coated surface formed by a smooth layer of oleic acid molecules. The thicknesses determined by ellipsometry indicate that if there is an underlying layer, it must be very thin, on the order of a few Å. However, if there were a layer of oleic acid, we would expect the contact angle of water to be large, even at low coverages. We find that the contact angle of water scales approximately as the thickness of the coating, as measured with ellipsometry. This result is thus consistent with a model in which the islands form on the bare silica substrate with the surface increasing in hydrophobicity as more of the silica sites are covered.

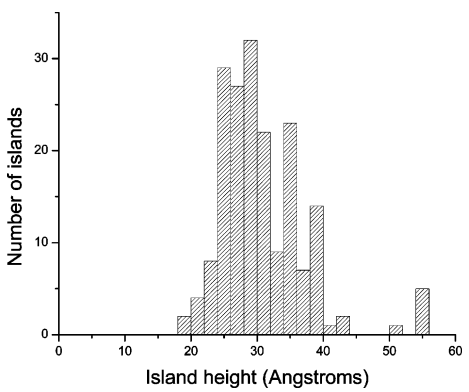

Fig. 4 Histogram of island heights on a 25 μm^2 region of a sample after a 17.5 h oleic acid deposition. Bin size is 2 Å.

Oleic acid coatings on polystyrene surfaces

AFM images of the bare polystyrene surface (coated on silica) and of oleic acid vapor-deposited on the polystyrene surface are shown in Fig. 5. As with the silica substrate, the AFM images show that the oleic acid is forming islands on the surface. Thus, we conclude that oleic acid forms islands when vapor-deposited onto both polar (silica) and nonpolar (polystyrene) surfaces.

Ellipsometry measurements of oleic acid deposition on the polystyrene showed that oleic acid thickness increases with deposition time, similar to the results obtained on silica. The contact angle of water on the bare polystyrene surface is approximately 45°, which is similar to the contact angle for the highest oleic acid coating on the silica surface. As the coating of oleic acid increases on the polystyrene surface, we observe no change in the contact angle. This result demonstrates that the hydrophobicities of the bare polystyrene surface and of the oleic acid islands on polystyrene surface are similar.

Because the contact-angle measurements do not change as a function of coating on the polystyrene surface, it is difficult to establish whether there is a monolayer of oleic acid lying flat on the surface under the islands. It is possible that formation of an oleic acid monolayer would be more favorable on the polystyrene surface compared to the silica surface because the long nonpolar hydrocarbon tail of the oleic acid would have favorable interactions with the nonpolar polystyrene surface.

Conclusions

We have investigated the vapor deposition of oleic acid onto silica and polystyrene surfaces, and we find that the rate of deposition slows with increasing deposition time on both surfaces at low coverages of oleic acid. This suggests that the oleic acid molecules are physisorbed on these surfaces and that re-evaporation is contributing to the non-linearity of the plot of adsorbate thickness as a function of time.

We further find that oleic acid forms islands on both silica and polystyrene surfaces. Oleic acid is known to exist as a dimer in the lengthwise direction in solution (Fig. 6).[32] Our observation that the average height of the oleic acid islands is approximately the length of one oleic acid molecule suggests that individual oleic acid molecules are oriented vertically on the surface. The contact-angle measurements show that the surface is hydrophobic at high coverages of oleic acid, suggesting that the hydrocarbon chain on the oleic acid molecule is facing away from the surface, as depicted in Fig. 6. The formation of strong hydrogen bonds between adjacent oleic acid groups, as well as dispersion forces along the alkane chain are the likely the energetic driving forces for island formation. The rate of formation and geometry of the islands are similar

Table 1 Statistics of oleic acid island formation on silica and polystyrene as a function of deposition time. The data indicate that as the deposition time increases, the number of islands increases, but their average height remains constant

	Silica surface			Polystyrene surface		
	10 min	40 min	17.5 h	6 min	22 min	98 min
Total number of islands in 25 μm^2	73	136	185	10	146	165
Mean $\pm$ standard deviation of island height/Å	29 $\pm$ 8	24 $\pm$ 8	31 $\pm$ 7	28 $\pm$ 8	27 $\pm$ 11	28 $\pm$ 15

on both the silica and polystyrene surfaces. This suggests that there are no fundamental differences in oleic acid surface mobility, which may be influenced by the orientation of the carboxylic acid group of oleic acid. An intriguing issue, for which we have no ready explanation, is that deposition proceeds by the formation of new islands and that "mature islands" stop growing beyond a diameter of about 100 nm. Island size can be predicted with Young's equation by balancing intermolecular forces and substrate-molecule forces, and so it is interesting that island size of oleic acid is similar on surfaces of very different polarities.

"Islanding" of organic coatings on substrates has been reported by other authors.[26] For example, Benitez, Salmeron *et al.*[26] found that solutions of octadecylamine in chloroform deposited onto mica formed islands with a height corresponding to molecules tilted at 49°. They found that the nature of the islands was highly dependent on factors such as the time of interaction, ripening time, humidity and amount of rinsing with the solvent. Our vapor-deposition method of preparation eliminates many of these variables that may affect the details of the island formation.

As mentioned in the Introduction, the studies presented here were originally motivated by unexpected preliminary observations of the aerodynamic diameter and the ozonolysis rate of particles coated with oleic acid. Based on the surface studies described here, we can now examine how the structure of oleic acid on aerosol particle surfaces may affect aerodynamic diameter and kinetics. First, we note that the aerodynamic diameter (d_a) is related to the volume-equivalent diameter (d) by the formula $d_a = d(\rho_a/\rho\chi)^{1/2}$, where ρ_a is the density of the particle, ρ is unit density and χ is the shape factor, defined as the ratio of resistance drag of the particle to that of a sphere having the same volume.[34] χ is 1 for a spherical particle, and is greater than one for a nonspherical particle (such as with island formation on a spherical core). Thus, for a constant coverage, a larger χ would result in a lower d_a.[23] Second, we consider the effect of surface structure on kinetics. If there is a thermodynamically preferred island size, then an increase in coverage should not result in a change in kinetics, for a pseudo-first order reaction with ozone in excess. Our results show that on flat substrates, as the amount of coverage increases, the average sizes (height and diameter) of the individual islands do not change. Therefore, we would expect the rate of ozonolysis to remain constant with increasing coverage.

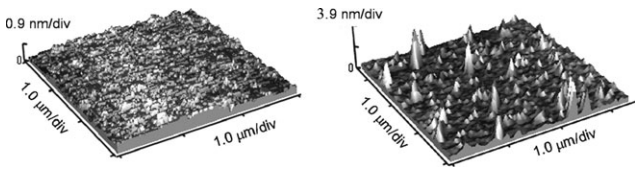

Fig. 5 Polystyrene spin-coated on silica (left) and oleic acid deposited on spin-coated polystyrene (right).

Atmospheric relevance

Our results are relevant to conditions that exist in the atmosphere. The process of oleic acid condensing onto dry inorganic substrates (such as dust or soot) in the boundary layer is well-mimicked by our vapor-deposition techniques. Oleic acid is released into the atmosphere from meat cooking, which occurs at elevated temperatures. As the temperature of the oleic acid decreases, its volatility decreases until it either homogeneously nucleates or is adsorbed onto a particle. Solid particles such as soot and dust represent a large fraction of the available surface area in the boundary layer on which low volatility organic species may condense. Thus, it is likely that oleic acid in the atmosphere condenses onto mineral dust or soot and the oleic acid may arrange itself in islands on these surfaces. Island formation may depend on both particle size and on the amount of coating (monolayer or multilayer). It is also possible that the surface structure of the oleic acid would be different when it is part of the large mixture of compounds present under typical atmospheric conditions.

While several studies have investigated the hygroscopicity of particles containing organic coatings,[35,36] few have addressed

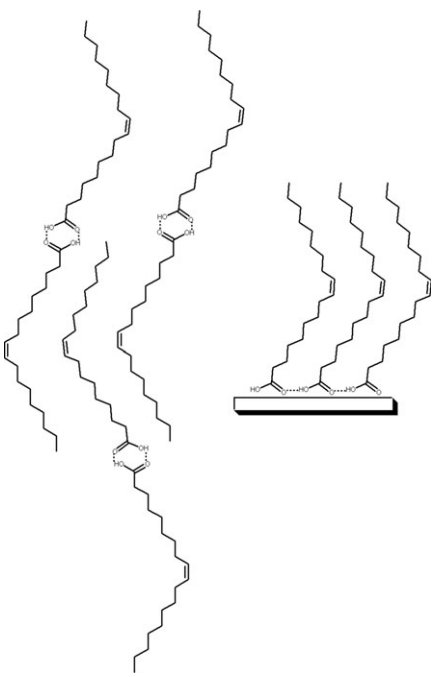

Fig. 6 Dimeric structure of oleic acid (left). Possible orientation of oleic acid on silica and polystyrene surfaces (right).

the role of surface morphology. When islands form, both the organic compound and the inorganic core particle are exposed to water vapor in the atmosphere. Mochida *et al*. have shown that CCN ability is directly related to the hygroscopicity of particles.[37] Thus, the CCN ability of the particle may be quite different when island formation occurs compared to when a particle is evenly coated. Oleic acid is one of many monocarboxylic and dicarboxylic acids detected in aerosols. We anticipate that deposition of other organic acids onto inorganic substrates may also result in island formation.

Acknowledgements

We thank Ms Laura Guy for help in collecting AFM images and Prof. Robert Nemanich and Jack Rowe for use of their AFM. We also gratefully acknowledge financial support to UNC for this project from the National Science Foundation.

References

1 L. M. Russell, S. F. Maria and S. C. B. Myneni, *Geophys. Res. Lett*., 2002, **29**, 1779.
2 H. Tervahattu, J. Juhanoja, V. Vaida, A. F. Tuck, J. V. Niemi, K. Kupiainen, M. Kulmala and H. Vehkamaki, *J. Geophys. Res., [Atmos.]*, 2005, **110**, D06207.
3 M. Mochida, N. Umemoto, K. Kawamura, H. J. Lim and B. J. Turpin, *J. Geophys. Res., [Atmos.]*, 2007, **112**, D15209.
4 P. R. Buseck and M. Posfai, *Proc. Natl. Acad. Sci. U. S. A*., 1999, **96**, 3372–3379.
5 M. Kanakidou, J. H. Seinfeld, S. N. Pandis, I. Barnes, F. J. Dentener, M. C. Facchini, R. Van Dingenen, B. Ervens, A. Nenes, C. J. Nielsen, E. Swietlicki, J. P. Putaud, Y. Balkanski, S. Fuzzi, J. Horth, G. K. Moortgat, R. Winterhalter, C. E. L. Myhre, K. Tsigaridis, E. Vignati, E. G. Stephanou and J. Wilson, *Atmos. Chem. Phys*., 2005, **5**, 1053–1123.
6 T. Anttila, A. Kiendler-Scharr, T. F. Mentel and R. Tillmann, *J. Atmos. Chem*., 2007, **57**, 215–237.
7 D. J. Donaldson and V. Vaida, *Chem. Rev*., 2006, **106**, 1445–1461.
8 A. H. Falkovich, G. Schkolnik, E. Ganor and Y. Rudich, *J. Geophys. Res., [Atmos.]*, 2004, **109**, D02208.
9 J. H. Seinfeld and S. N. Pandis, *Atmospheric Chemistry and Physics: From Air Pollution to Climate Change*, John Wiley & Sons Inc., New York, 2nd edn, 2006.
10 Y. Rudich, N. M. Donahue and T. F. Mentel, *Annu. Rev. Phys. Chem*., 2007, **58**, 321–352.
11 T. Thornberry and J. P. D. Abbatt, *Phys. Chem. Chem. Phys*., 2004, **6**, 84–93.
12 J. A. Thornton and J. P. D. Abbatt, *J. Phys. Chem. A*, 2005, **109**, 10004–10012.
13 J. Q. Xiong, M. H. Zhong, C. P. Fang, L. C. Chen and M. Lippmann, *Environ. Sci. Technol*., 1998, **32**, 3536–3541.
14 G. B. Ellison, A. F. Tuck and V. Vaida, *J. Geophys. Res., [Atmos.]*, 1999, **104**, 11633–11641.
15 N. Rontu and V. Vaida, *J. Phys. Chem. C*, 2007, **111**, 11612–11618.
16 J. W. Morris, P. Davidovits, J. T. Jayne, J. L. Jimenez, Q. Shi, C. E. Kolb, D. R. Worsnop, W. S. Barney and G. Cass, *Geophys. Res. Lett*., 2002, **29**, 1357.
17 G. D. Smith, E. Woods, C. L. DeForest, T. Baer and R. E. Miller, *J. Phys. Chem. A*, 2002, **106**, 8085–8095.
18 Y. Katrib, G. Biskos, P. R. Buseck, P. Davidovits, J. T. Jayne, M. Mochida, M. E. Wise, D. R. Worsnop and S. T. Martin, *J. Phys. Chem. A*, 2005, **109**, 10910–10919.
19 D. G. Nash, M. P. Tolocka and T. Baer, *Phys. Chem. Chem. Phys*., 2006, **8**, 4468–4475.
20 G. Blyholder, C. Adhikar and A. Proctor, *Colloids Surf., A*, 1995, **105**, 151–158.
21 Z. W. Li and Y. F. Zhu, *Appl. Surf. Sci*., 2003, **211**, 315–320.
22 P. Liu, P. J. Ziemann, D. B. Kittelson and P. H. Mcmurry, *Aerosol Sci. Technol*., 1995, **22**, 293–313.
23 Y. Katrib, S. T. Martin, Y. Rudich, P. Davidovits, J. T. Jayne and D. R. Worsnop, *Atmos. Chem. Phys*., 2005, **5**, 275–291.
24 Y. Katrib, S. T. Martin, H. M. Hung, Y. Rudich, H. Z. Zhang, J. G. Slowik, P. Davidovits, J. T. Jayne and D. R. Worsnop, *J. Phys. Chem. A*, 2004, **108**, 6686–6695.
25 N. P. Levitt, R. Y. Zhang, H. X. Xue and J. M. Chen, *J. Phys. Chem. A*, 2007, **111**, 4804–4814.
26 J. J. Benitez, S. Kopta, D. F. Ogletree and M. Salmeron, *Langmuir*, 2002, **18**, 6096–6100.
27 T. A. Mykhaylyk, N. L. Dmitruk, S. D. Evans, I. W. Hamley and J. R. Henderson, *Surf. Interface Anal*., 2007, **39**, 575–581.
28 X. S. Hu, K. Shin, M. Rafailovich, J. Sokolov, R. Stein, Y. Chan, K. Williams, W. L. Wu and R. Kolb, *High Perform. Polym*., 2000, **12**, 621–629.
29 M. J. Frisch, G. W. Trucks, H. B. Schlegel, G. E. Scuseria, M. A. Robb, J. R. Cheeseman, J. A. Montgomery, Jr., T. Vreven, K. N. Kudin, J. C. Burant, J. M. Millam, S. S. Iyengar, J. Tomasi, V. Barone, B. Mennucci, M. Cossi, G. Scalmani, N. Rega, G. A. Petersson, H. Nakatsuji, M. Hada, M. Ehara, K. Toyota, R. Fukuda, J. Hasegawa, M. Ishida, T. Nakajima, Y. Honda, O. Kitao, H. Nakai, M. Klene, X. Li, J. E. Knox, H. P. Hratchian, J. B. Cross, V. Bakken, C. Adamo, J. Jaramillo, R. Gomperts, R. E. Stratmann, O. Yazyev, A. J. Austin, R. Cammi, C. Pomelli, J. Ochterski, P. Y. Ayala, K. Morokuma, G. A. Voth, P. Salvador, J. J. Dannenberg, V. G. Zakrzewski, S. Dapprich, A. D. Daniels, M. C. Strain, O. Farkas, D. K. Malick, A. D. Rabuck, K. Raghavachari, J. B. Foresman, J. V. Ortiz, Q. Cui, A. G. Baboul, S. Clifford, J. Cioslowski, B. B. Stefanov, G. Liu, A. Liashenko, P. Piskorz, I. Komaromi, R. L. Martin, D. J. Fox, T. Keith, M. A. Al-Laham, C. Y. Peng, A. Nanayakkara, M. Challacombe, P. M. W. Gill, B. G. Johnson, W. Chen, M. W. Wong, C. Gonzalez and J. A. Pople, *GAUSSIAN 03 (Revision C.02)*, Gaussian, Inc., Wallingford, CT, 2004.
30 D. J. Rader, P. H. Mcmurry and S. Smith, *Aerosol Sci. Technol*., 1987, **6**, 247–260.
31 I. N. Tang and H. R. Munkelwitz, *J. Colloid Interface Sci*., 1991, **141**, 109–118.
32 M. Iwahashi, Y. Kasahara, H. Matsuzawa, K. Yagi, K. Nomura, H. Terauchi, Y. Ozaki and M. Suzuki, *J. Phys. Chem. B*, 2000, **104**, 6186–6194.
33 A. Kubono, N. Yuasa, H. L. Shao, S. Umemoto and N. Okui, *Appl. Surf. Sci*., 2002, **193**, 195–203.
34 W. C. Hinds, *Aerosol Technology: Properties, Behavior, and Measurement of Airborne Particles*, Wiley-Interscience, New York, 1999.
35 C. N. Cruz and S. N. Pandis, *J. Geophys. Res., [Atmos.]*, 1998, **103**, 13111–13123.
36 J. E. Shilling, S. M. King, M. Mochida and S. T. Martin, *J. Phys. Chem. A*, 2007, **111**, 3358–3368.
37 M. Mochida, M. Kuwata, T. Miyakawa, N. Takegawa, K. Kawamura and Y. Kondo, *J. Geophys. Res., [Atmos.]*, 2006, **111**, D23206.